

Features of the Temperature Dependence of the Specific Contact Resistance of Au–Ti–Pd– n^+ – n -Si Diffusion Silicon Structures

A. E. Belyaev^a, N. S. Boltovets^b, V. P. Klad'ko^a, N. V. Safryuk-Romanenko^a, A. I. Lubchenko^a,
V. N. Sheremet^a, V. V. Shynkarenko^{a,*}, A. S. Slepova^b, V. A. Pilipenko^c,
T. V. Petlitskaya^c, A. S. Pilipchuk^d, R. V. Konakova^a, and A. V. Sachenko^a

^a Lashkaryov Institute of Semiconductor Physics, National Academy of Sciences of Ukraine, Kyiv, 03028 Ukraine

^b State Enterprise Research Institute “Orion”, Kyiv, 03057 Ukraine

^c OAO “INTEGRAL”—Holding Management Company, Minsk, 220108 Belarus

^d Institute of Physics, National Academy of Sciences of Ukraine, Kyiv, 03028 Ukraine

*e-mail: shynkarenko@gmail.com

Received October 23, 2018; revised November 6, 2018; accepted November 12, 2018

Abstract—The temperature dependences of the specific contact resistance of silicon ρ_c with a doping step are measured experimentally and described theoretically. The measurements are performed in the temperature range from 4.2 to 380 K. It is established that the contacts of the studied Au–Ti–Pd– n^+ – n -Si structures are ohmic. It is shown that minimal ρ_c is implemented at $T = 75$ K. Its value rises both with a decrease in temperature (due to the freezing effect) and with an increase in temperature (due to the electron-enriched layer at the boundary with the bulk material). It is established that the bulk electron concentration strongly decreases in the near-contact region in a layer with a thickness on the order of one micron due to the compensation of silicon by deep acceptors appearing because of the formation of a rather high vacancy concentration during stress relaxation and the appearance of a high dislocation density, as well as due to their diffusion from the contact after heating to 450°C. The data on the occurrence of vacancy-type defects are confirmed by X-ray measurements. The dislocation density in the studied structures is also estimated from X-ray measurements.

DOI: 10.1134/S1063782619040055

1. INTRODUCTION

Up to now, scientific notions on ohmic contacts to semiconductors were based on the theory of the metal–semiconductor contact [1]. A low-barrier Schottky contact with an electron work function from the metal that is lower than the electron work function from the semiconductor is considered in the case of an n -type semiconductor; the current–voltage characteristic of such a contact is linear and symmetric. Herewith, the specific contact resistance ρ_c decreases with an increase in temperature for the thermionic and thermal-field current-transfer mechanisms in the contact and is temperature-independent for the tunneling mechanism.

However, there are experimental works on the investigation into ohmic contacts, in which an increase in ρ_c with an increase in temperature is observed, not described by known theoretical models [2, 3].

We proposed and experimentally confirmed a model for the formation of an ohmic contact explaining the increase in ρ_c with an increase in temperature in ohmic contacts to single-crystalline n^+ -Si with a

doping level of silicon of $\sim 10^{19}$ cm $^{-3}$ by means of current passage through metallic shunts combined with dislocations, near the ends of which (shunts) enriching band bending appears. A current-transfer mechanism which is nonbarrier in principle is implemented in this case [4, 5]. The nature of dislocations appearing in the near-contact region is most often associated with the relaxation of mechanical stresses in the contact. This was shown by the example of alloy contacts to Si, III–V compounds [6], or ohmic contacts to trinitride heterostructures [7] grown on foreign substrates. The dislocation density in such heterostructures is 10^7 – 10^{11} cm $^{-2}$ for various types of device structures. The dislocation density in ohmic contacts to Si and III–V compounds reaches 10^8 cm $^{-2}$.

It is known that the ohmic contact in modern semiconductor devices is formed to a specially doped n^+ layer (or p^+ layer), to a so-called doping step formed by diffusion, ion doping, or epitaxy. The generation of structural defects in this layer depending on the doping level and their role in the formation and properties of ohmic contacts have not been investigated in detail. At the same time, knowledge of the dependence $\rho_c(T)$

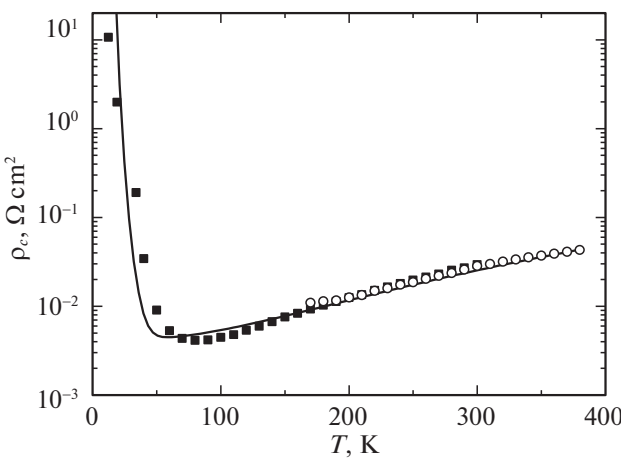


Fig. 1. Experimental and theoretical dependences $\rho_c(T)$ for silicon with a doping step. $n_2 = 1.6 \times 10^{13} \text{ cm}^{-3}$, $A^* = 112 \text{ A cm}^{-2} \text{ K}^{-2}$, and $N_c = 2.8 \times 10^{19} \text{ cm}^{-3}$.

for devices, whose operating temperatures exceed 300 K, is necessary. This is associated with the fact that an increase in ρ_c leads to worsening of their parameters, for example, it lowers the efficiency and figure of merit of microwave diodes [8]. The values of ρ_c at liquid-helium temperatures is also of interest, for example, for temperature sensors [9] and other devices of cryogenic electronics [10]. Therefore, both experimental and theoretical investigations into the $\rho_c(T)$ dependence in ohmic contacts and the specifics of structural defects in the near-contact layer seem to be topical.

Since the electrical, structural, and mechanical properties of silicon are well studied and it is still the main semiconductor material of the electronics industry, we select specifically ohmic contacts with a doping step in Si as the model ones for investigating the features of the temperature dependence of ρ_c .

2. EXPERIMENTAL

In this work, the doping step was formed by the diffusion of phosphorus into an n -type (100) silicon wafer with $\rho = 7.5 \Omega \text{ cm}$, a thickness of 400 μm , and a dislocation density of $\sim 10^5 \text{ cm}^{-2}$. The diffusion layer depth was 0.5 μm . Diffusion was performed at $T = 900, 925, 950$, and 970°C [11].

The specific contact resistance of Au(150 μm)–Ti(60 nm)–Pd(20 nm)– n^+ – n -Si ohmic contacts was measured in the vertical geometry in the temperature range of 4.2–300 K for test structures assembled in a case.

The Au, Ti, and Pd films were formed by the vacuum sputtering of metals in one process cycle on a substrate heated to 350°C . The Pd_2Si -based ohmic contact was formed immediately during sputtering.

The contacts were burned-in at $T = 350^\circ\text{C}$ (the samples underwent diffusion at $T = 900^\circ\text{C}$ and 925°C) and $T = 450^\circ\text{C}$ (the samples underwent diffusion at $T = 950^\circ\text{C}$ and 970°C) at a residual pressure of 10^{-4} Pa for 10 min [11]. The structural quality of the samples was investigated by high-resolution X-ray diffractometry using a Panalytical X'Pert PRO MRD diffractometer [11, 12].

3. RESULTS OF MEASUREMENTS OF ρ_c AND THEIR DISCUSSION

The temperature dependences of ρ_c were measured for test TLM structures. The typical dependence $\rho_c(T)$ measured in the temperature range 12.5–400 K is presented in Fig. 1. It is seen that a minimum at $T = 75 \text{ K}$ is observed in the $\rho_c(T)$ dependence. On both sides of the minimum, ρ_c increases more rapidly with a decrease in temperature, i.e., $\rho_c(T)$ differs from the dependences $\rho_c(T)$ predicted by theory [1]. Herewith, neither the thermionic current-transport mechanism nor the thermal-field mechanism explains the $\rho_c(T)$ dependence at liquid-helium temperatures.

Let us consider the model of an ohmic contact with a doping step in the near-contact region when electron degeneracy occurs in a heavily doped n^+ layer. Just this case is implemented in the technology of silicon semiconductor devices including avalanche diodes. Herewith, the thickness of the heavily doped W_{n^+} region with an electron concentration of n_l^+ exceeds the thickness of the Schottky layer W_{Sch} , while the doping level is higher than the effective density of states of electrons in the conduction band N_c . Precisely this fact means that electron degeneracy occurs in the heavily doped region.

In this work, we performed analytical calculation of the $\rho_c(T)$ dependence for ohmic contacts with a doping step based on Si for the limiting case when the band diagram has the form presented in Fig. 2.

It is seen from Fig. 2 that the thickness of the heavily doped region W_{n^+} with an electron concentration of n_l^+ exceeds the thickness of the Schottky layer W_{Sch} in the case under consideration, i.e., $W_{n^+} > W_{\text{Sch}}$, while the doping level is higher than the effective density of states of electrons in the conduction band N_c , i.e., $n_l^+ > N_c$. This fact means that electron degeneracy occurs in the heavily doped region. The bulk electron concentration in the lightly doped region herewith equals n_2 .

In this case, the specific contact resistance can be presented in the form of the in-series connection of two resistances:

$$\rho_c = \rho_{c1} + \rho_{c2}, \quad (1)$$

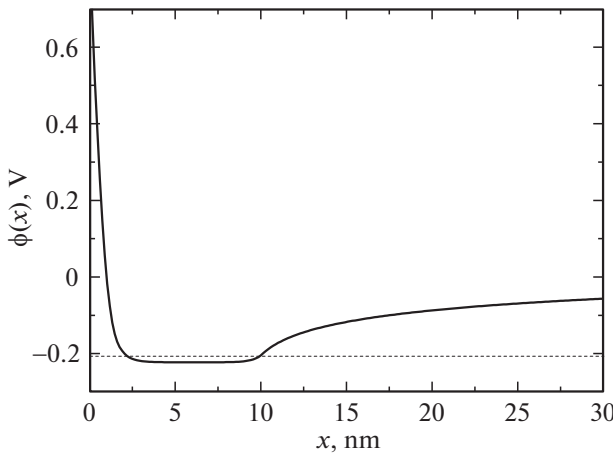


Fig. 2. Band diagram of the ohmic contact with a doping step of the n^+ - n -type with the parameters: $n^+ \sim 5 \times 10^{20} \text{ cm}^{-3}$, $n_2 \sim 10^{15} \text{ cm}^{-3}$, and $W_{n^+} \sim 0.01 \mu\text{m}$.

where ρ_{c1} is the specific contact resistance associated with the thermal-field electron passage through the barrier at the boundary of the heavily doped semiconductor and metal, while

$$\rho_{c2} = \frac{kN_c}{qA^*Tn_2} \left(1 + \frac{L_D A^* T}{k\mu_n N_c} \right) \quad (2)$$

is the effective specific contact resistance of the lightly doped region in the limiting case, when the energy diagram of the contact has the form presented in Fig. 2. Here, q is the elementary charge, k is the Boltzmann constant, A^* is the effective Richardson constant, μ_n is the electron mobility in the lightly doped region, and $L_D = (\epsilon_0 \epsilon_s kT / 2q^2 n_2)^{0.5}$ is the Debye screening length for the lightly doped region.

We note that expression (2) is derived allowing for the results of [13] and [14], i.e., it takes into account both the diffusion and emission summands in the current flowing through the lightly doped region.

Thus, if equality $\rho_{c2} > \rho_{c1}$ is fulfilled, the contact is purely ohmic. In this case, the band bending in the doped region is not depleting but enriching; and therefore, the entire voltage supplied to the object will drop at the neutral bulk, which is precisely what provides the ohmic character of the contact.

The electron mobility μ_n in the lightly doped region was calculated allowing for scattering at charged impurities as well as at intervalley and acoustic phonons [15]. It was assumed that the dislocation density in the lightly doped region is rather low and does not affect the electron mobility. The expressions for the calculation of μ_n are presented in [16].

Let us further turn our attention to the analysis of the temperature dependence of the resistance ρ_{c2} . If the role of the diffusion current is small, i.e., inequality $(L_D A^* T / k\mu_n N_c) < 1$ is fulfilled, the tem-

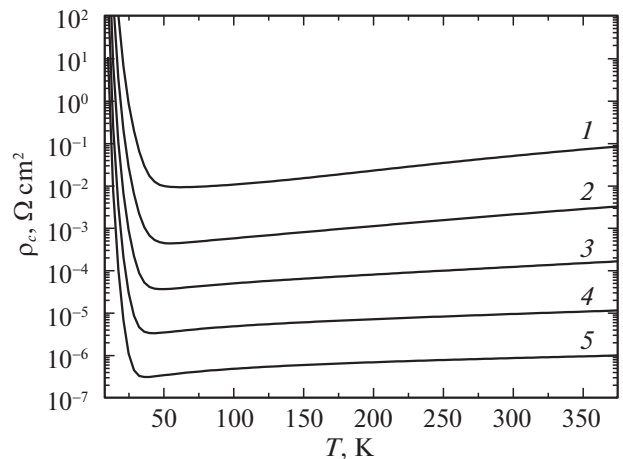


Fig. 3. Theoretical dependences using formula (2) and allowing for the low-temperature freezing of electrons n_2 : (1) 10^{13} , (2) 10^{14} , (3) 10^{15} , (4) 10^{16} , (5) 10^{17} cm^{-3} , $A^* = 112 \text{ A cm}^{-2} \text{ K}^{-2}$, $N_c = 2.8 \times 10^{19} \text{ cm}^{-3}$.

perature dependence of ρ_{c2} allowing for the fact that $N_c(T) = N_{c0}(T/300)^{3/2}$ has the form $\rho_{c2} \sim \sqrt{T}$, i.e., the specific contact resistance rises with an increase in temperature as \sqrt{T} . It was shown in [13] that this inequality is fulfilled in the region of doping levels when $n_2 \gg 10^{15} \text{ cm}^{-3}$. In the region of low and intermediate doping levels, $(L_D A^* T / k\mu_n N_c) \geq 1$ and the analysis shows that the degree of an increase in ρ_{c2} with rising temperature increases when compared with law T .

Figure 3 shows the theoretical dependences of $\rho_{c2}(T)$ using formula (2) as well as the low-temperature freezing of electrons when it is taken into account that the electron concentration in the semiconductor bulk $n_2(T)$ is determined upon using the neutrality equation of the form

$$\frac{N_d}{1 + \exp((E_F - E_d)/kT)} = \frac{2}{\sqrt{\pi}} N_{c0} \left(\frac{T}{300} \right)^{3/2} \times \int_0^\infty \frac{\kappa^{0.5}}{1 + \exp(\kappa - E_F/kT)} d\kappa, \quad (3)$$

where E_d is the energy of shallow donor levels, E_F is the Fermi energy, N_{c0} is the effective density of states in the conduction band at $T = 300 \text{ K}$, and κ is the kinetic energy of electrons in the conduction band normalized to kT .

The parameter of the curves is the doping level. All dependences have a growing character in the temperature region higher than 80 K. In the case of curve 1, which corresponds to the lowest doping level of 10^{13} cm^{-3} , the degree of the rise of $\rho_{c2}(T)$ in the region of elevated temperatures is highest and equals 2.4.

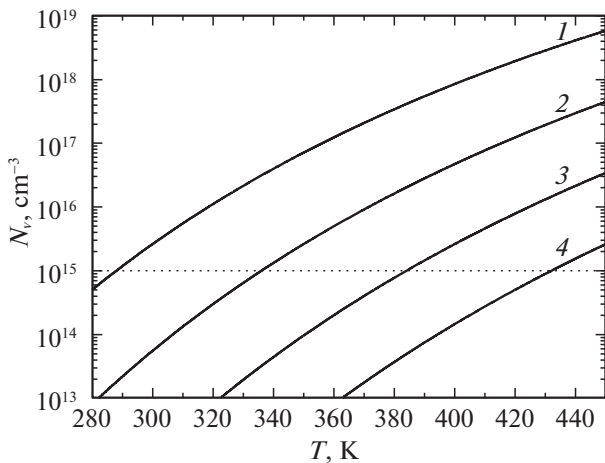


Fig. 4. Dependences of the vacancy concentration N_v on temperature (4). $A = 10^{23} \text{ cm}^{-3}$, $F = 3 \times 10^3$, and W : (1) 0.6, (2) 0.7, (3) 0.8, and (4) 0.9 eV.

It decreases with an increase in the doping level and equals, respectively: 2.1 for $n_2 = 10^{14} \text{ cm}^{-3}$, 1.4 for $n_2 = 10^{15} \text{ cm}^{-3}$, 1 for $n_2 = 10^{16} \text{ cm}^{-3}$, and 0.8 for $n_2 = 10^{17} \text{ cm}^{-3}$.

Let us return to Fig. 1. It shows the experimental dependences $\rho_c(T)$ found for Si samples with a doping step, formed by phosphorus diffusion to a depth of 0.2 μm . They were measured twice starting from liquid-helium temperatures, notably, from 12.5 to 300 K, as well as from liquid-nitrogen temperatures, notably, from 170 to 380 K. It is seen from Fig. 1 that the experimental curves agree well with one another in the region $T \geq 170$ K. The theoretical curve is plotted according to formula (2), in which low-temperature carrier freezing is taken into account. However, it should be noted that agreement is found when using a bulk concentration in silicon of $1.6 \times 10^{13} \text{ cm}^{-3}$, while the initial doping level was $\sim 10^{15} \text{ cm}^{-3}$.

We can explain such a decrease in the bulk electron concentration if we assume that extended and point defects with rather high concentrations of deep acceptor levels appear in the n -Si substrate because of the relaxation of mechanical stresses. For this reason, a compensated layer emerges between the heavily doped layer and the substrate [17]. In addition, palladium, which is included in the contact system, also possesses acceptor properties and forms acceptor centers in Si [18, 19]. The introduction of Pd into n -Si leads either to a decrease in the electron concentration, i.e., partial compensation at $N_d > N_{\text{Pd}}$, or to a change in the conduction type (at $N_{\text{Pd}} > N_d$) [17, 18], i.e., when doping with Pd, we can compensate the conductivity of low-ohmic Si to the intrinsic one [17]. For this reason, it is quite possible to decrease the electron concentration in the n -Si substrate and increase ρ_c as a result of this.

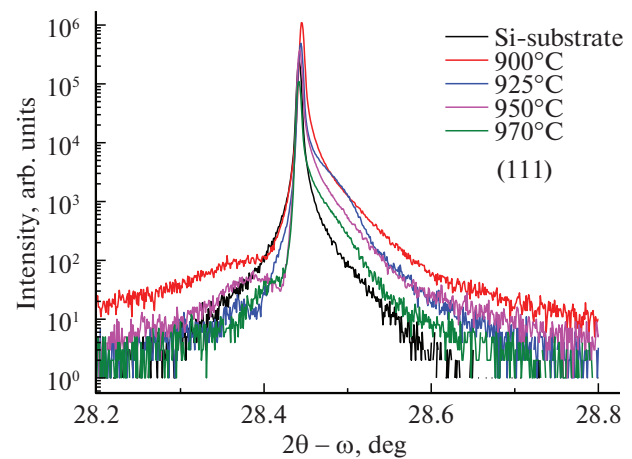


Fig. 5. $20-\omega$ scan of the asymmetric silicon (111) reflection.

The acceptor nature of the centers is also evidenced by a high concentration of vacancies in silicon after heat treatment of the contact systems. Indeed, the vacancy concentration N_v in Si is determined according to the data of [17, 20, 21] as

$$N_v = AF \exp(-W/kT), \quad (4)$$

where W —the formation energy of vacancies in Si—varies depending on the doping level of silicon with phosphorus from 4 to 0.6 eV, decreases with an increase in the concentration of the doping impurity to $\sim 10^{20} \text{ cm}^{-3}$, and leads to a decrease in the equilibrium vacancy concentration by ~ 2 orders of magnitude due to ion–phosphorus vacancy complex formation [21, 22]. The appearance of local elastic stresses in the Si lattice due to the difference in the atomic radii of the impurity (Pd) and matrix (Si) also leads to a decrease in W . Compressive stresses arise around the impurity atoms at $R_{\text{Pd}} > R_{\text{Si}}$. This should decrease W , increase the equilibrium vacancy concentration, and decrease the concentration of interstitial atoms. Indeed, $R_{\text{Pd}} = 0.137 \text{ nm}$, while $R_{\text{Si}} = 0.117 \text{ nm}$, $R_{\text{Pd}} > R_{\text{Si}}$, which should lead to stresses around the impurity (Pd) and, consequently, a decrease in W [23]. Here, A is the proportionality coefficient, which depends on the number of atoms in the volume unit of the crystal and on the number of vacant places, α which the atom can jump. F is a function that gradually varies with temperature, the numerical value of which in terms of order of magnitude lies in the limits of 10^3 – 10^4 .

For the set of different values of W , the dependence of the vacancy concentration N_v on temperature T will be determined by the dependences (4) presented in Fig. 4. It is seen from Fig. 4 that the vacancy concentration at vacancy energies lying in the range of 0.6–0.9 eV and temperatures exceeding 280°C varies in broad limits and can exceed 10^{18} cm^{-3} . Such a vacancy concentration is sufficient for the almost complete

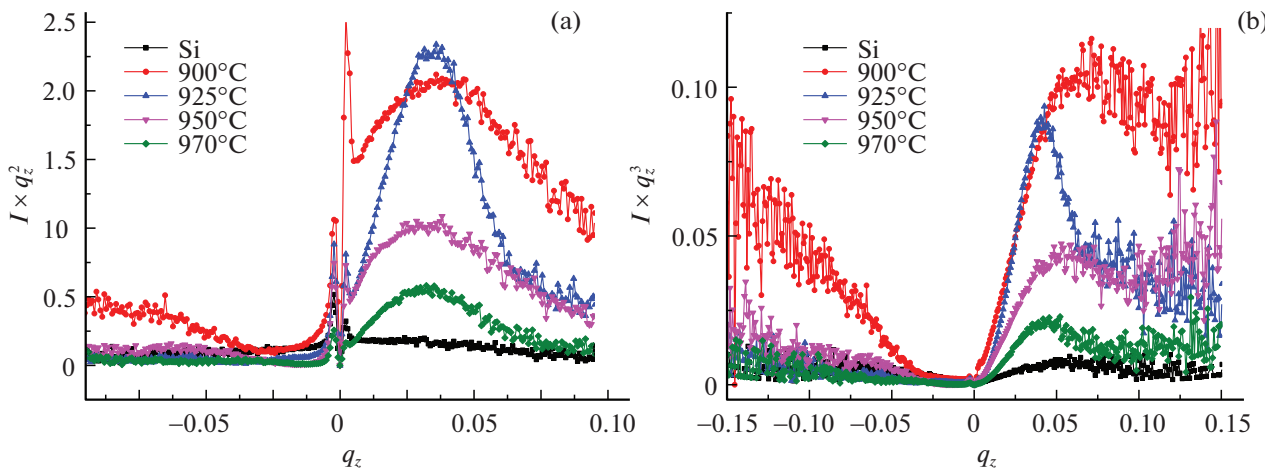


Fig. 6. Comparison of the constructions (a) $I = Iq_z^2$ and (b) $I = Iq_z^3$ found from the $2\theta-\omega$ scans.

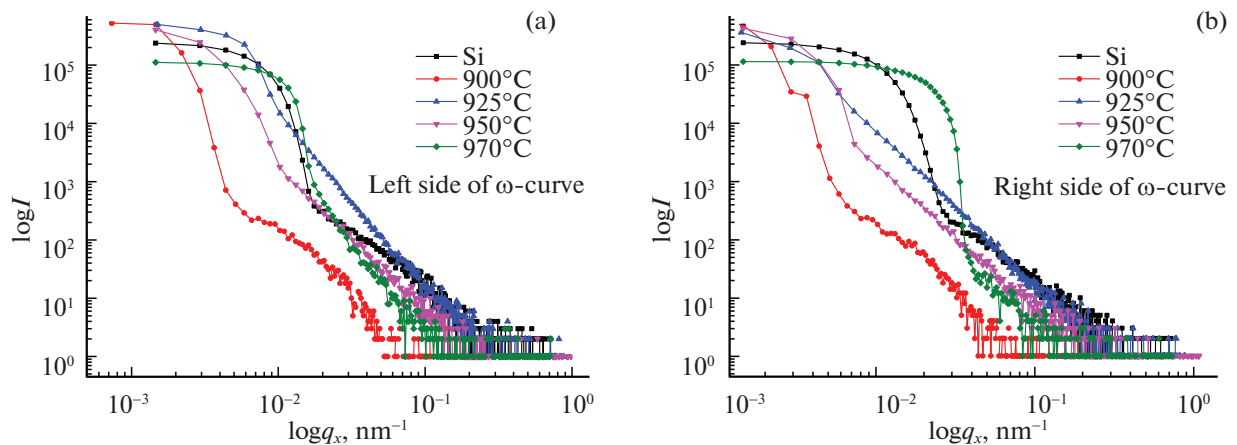


Fig. 7. Left (a) and right (b) sides of the ω scans directed perpendicular to the diffraction vector and reconstructed in coordinates $\log I / (\log q_x)$.

compensation of silicon including heavily doped silicon. To confirm these assumptions, we performed X-ray structural investigations of these samples.

4. STRUCTURAL INVESTIGATIONS

To determine the defect state of the samples, we measured ω - and $\omega-2\theta$ scans for symmetric reflections (111). It is seen from Fig. 5 that the full-width at half-maximum of the diffraction reflection curve (DRC) increases, and also the intensity of diffusion scattering or “tails” on both sides of the DRC maximum grow. A decrease in the diffusion scattering tails on both sides of the DRC maximum is observed with an increase in the diffusion temperature to 925°C. The subsequent increase in the diffusion temperature leads to the strongest DRC asymmetry, and the diffusion component on the side of large angles is dominant.

To analyze the DRCs, we used the relationships for the transformation of angular coordinates in reciprocal lattice space:

$$\begin{aligned} \frac{q_x}{2\pi} &= \frac{1}{\lambda}(\cos \omega - \cos(2\omega' - \omega)) \Rightarrow q_x \\ &= \frac{2\pi}{\lambda}(\cos \omega - \cos(2\omega' - \omega)), \end{aligned} \quad (5)$$

$$\begin{aligned} \frac{q_z}{2\pi} &= \frac{1}{\lambda}(\sin \omega - \sin(2\omega' - \omega)) \Rightarrow q_z \\ &= \frac{2\pi}{\lambda}(\sin \omega - \sin(2\omega' - \omega)). \end{aligned} \quad (6)$$

Here, λ is the X-ray radiation wavelength, which corresponds to $\text{Cu}K_{\alpha}$; q_x and q_z are the coordinates in reciprocal lattice space; and ω and ω' are the incidence and reflection angles, respectively.

Table 1. Estimation of the sizes of defect regions

Sample diffusion T , °C	Sizes of regions of vacancy defects, nm		Sizes of regions of interstitial defects, nm	
	from Iq_z^2	from Iq_z^3	from Iq_z^2	from Iq_z^3
Si (initial)	27.1	1.2	15.6	1.3
900	97.5	6.3	88.9	8.1
925	16.4	3.3	—	2.5
950	19.7	3.1	42.5	3.7
970	25.7	5.7	21.4	2.5

To analyze the type of defects in the samples, we used high-resolution $2\theta-\omega$ and ω scans. The dependences $I = Iq_z^2$ and $I = Iq_z^3$ presented in Figs. 6a and 6b, respectively, were constructed from the $2\theta-\omega$ scans.

It is seen from the curves presented in Fig. 6 that defects of both the vacancy type ($q_z < 0$) and interstitial type ($q_z > 0$) are present in these samples. A decrease in the concentration of defects of both types is observed at a diffusion temperature of 900°C , although interstitial defects prevail. A decrease in the number of vacancy-type defects is observed with a further increase in temperature. The concentration of main defects of the type of interstitial atoms also has the tendency toward decay with an increase in the phosphorus diffusion temperature [24]. Such decay can be associated with an increase in the number of dislocations in the samples with an increase in the diffusion temperature [25].

Analysis of the ω scans recorded in the direction perpendicular to the diffraction vectors was performed with the help of constructions $\log I = f(\log q_x)$ presented in Figs. 7a and 7b, respectively. The size distributions of defects were found from the positions of the distribution maxima of the diffuse scattering of curves in Fig. 6 (Table 1). The dislocation density was estimated from the half-widths of the ω scans (Table 2). The estimations show that our results of the vacancy-

type and interstitial-type regions correspond to the data [26].

It is seen from Table 2 that the dislocation density in the initial wafer is $\sim 2.2 \times 10^5 \text{ cm}^{-2}$, which is typical of heavily doped Si [25, 27]. The variation in the dislocation density is observed as a result of an increase in the diffusion temperature due to the rise of mechanical stresses in the Si wafer. An increased vacancy concentration and decreased concentration of interstitial atoms appears in the compression region [25].

Then metal films were deposited onto these Si wafers: a Pd film 30 nm in thickness, a Ti film 60 nm in thickness, and a Au film 120 nm in thickness. The contact metallization was burned-in at $T = 350^\circ\text{C}$ (samples 900°C and 925°C) and $T = 450^\circ\text{C}$ (samples 950°C and 970°C) for 10 min. The dislocation density, the values of which are presented in Table 3, was determined for these samples.

We found the relative deformations in the samples that underwent diffusion with burned-in contacts (Table 4) by the peak shift from reflection (111) Si in the $2\theta-\omega$ scans and calculated the internal mechanical stresses σ from Tables 3 and 4 [28]. It is seen that low-temperature annealing leads to an increase in σ and the dislocation density when compared with the samples that underwent only diffusion. This evidences the substantial reconstruction of ensembles of point and linear defects as well as dislocation generation during low-temperature treatment. Herewith, defects, for the formation of which a lower energy consumption is required, will prevail.

Thus, it follows from the data that the compensation of silicon is associated with:

- (i) the diffusion of Pd at T_{ann} of 350°C or 450°C from the Au–Ti–Pd– n^+ – n -Si ohmic contact;
- (ii) a high density of point defects (vacancies) in Si appearing during heat treatment;
- (iii) a high dislocation density appearing during diffusion and heat treatment.

Table 2. Estimation of the dislocation density

Sample diffusion T , °C	Full-width at half-maximum (deg)	Dislocation density, cm^{-2}
Si (initial)	0.01033	2.20×10^5
900	0.00210	9.10×10^3
925	0.00529	5.77×10^4
950	0.00429	3.80×10^4
970	0.01799	6.68×10^5

Table 3. Estimation of the dislocation density

Sample diffusion <i>T</i> , °C	Annealing <i>T</i> **, °C	Full-width at half- maximum* (deg)	Full-width at half- maximum** (deg)	Dislocation density*, cm ⁻²	Dislocation density**, cm ⁻²
900	350	0.00210	0.02064	9.10×10^3	8.79×10^5
925	350	0.00529	0.00436	5.77×10^4	3.92×10^4
950	450	0.00429	0.00995	3.80×10^4	2.04×10^5
970	450	0.01799	0.00407	6.68×10^5	3.42×10^4

*Initial silicon wafer with formed an n^+ -Si layer and **the same sample after metallization and annealing.

Table 4. Calculation of the quantity σ according to the data [28] and ε

Sample diffusion <i>T</i> , °C	ε , %	$\sigma = \sigma_0 \varepsilon \times 100\%$, Pa ($\sigma_0 = 187.8 \times 10^9$ Pa [28])
Si	-1.44×10^{-5}	-2.70×10^6
900	-1.10×10^{-4}	-2.07×10^7
925	-8.33×10^{-5}	-1.56×10^7
950	-3.86×10^{-5}	-7.25×10^6
970	-1.36×10^{-4}	-2.55×10^7
With contacts		
900 (annealing at 350°C)	-3.41×10^{-5}	-6.40×10^6
925 (annealing at 1350°C)	-1.53×10^{-4}	-2.87×10^7
950 (annealing at 450°C)	-8.17×10^{-5}	-1.53×10^7
970 (annealing at 350°C)	-1.57×10^{-4}	-2.95×10^7

5. CONCLUSIONS

The data presented in our work and their analysis evidence that the studied Au–Ti–Pd– n^+ –*n*-Si silicon structures are ohmic contacts in the temperature range from 4.2 to 380 K. It is established that the specific contact resistance ρ_c in the region $T \geq 80$ K rises according to the power law upon an increase in temperature. The degree of the rise increases with a decrease in the bulk doping level from 0.8 at rather high doping levels ($\sim 10^{17}$ cm⁻³) to 2.4 at low doping levels ($\sim 10^{13}$ cm⁻³).

It is shown that compensation of the material bulk occurs in the intermediate layer between the heavily doped region and bulk. It is in particular associated with the formation of a high vacancy concentration due to the high dislocation density appearing during diffusion and heat treatment.

The formation of dislocations and vacancy-type defects is confirmed by the data of X-ray investigations.

REFERENCES

- S. M. Sze, *Physics of Semiconductor Devices* (Wiley, New York, 1981; Mir, Moscow, 1984), Vol. 1.
- S. E. Swirhun and R. M. Swanson, IEEE Electron Dev. Lett. **7**, 155 (1986).
- D. K. Schroder, *Semiconductor Material and Device Characterization*, 3rd ed. (IEEE, Wiley, New York, 2006).
- A. E. Belyaev, N. S. Boltovets, R. V. Konakova, Ya. Ya. Kudryk, A. V. Sachenko, and V. N. Sheremet, Semicond. Phys., Quantum Electron. Optoelectron. **13**, 436 (2010).
- A. V. Sachenko, A. E. Belyaev, V. A. Pilipenko, T. V. Petlitskaya, V. A. Anishchik, N. S. Boltovets, R. V. Konakova, Ya. Ya. Kudryk, A. O. Vinogradov, and V. N. Sheremet, Semiconductors **48**, 492 (2014).
- U. M. Kulish and A. P. Vyatkin, Izv. Vyssh. Uchebn. Zaved., Fiz. **6**, 157 (1965).
- A. E. Belyaev, V. N. Bessonov, N. S. Boltovets, Yu. V. Zhilyaev, V. P. Klad'ko, R. V. Konakova, A. V. Kuchuk, A. V. Sachenko, and V. N. Sheremet, *Physical and Technological Problems of Nitride Gallium Electronics* (Nauk. Dumka, Kiev, 2016) [in Russian].
- N. S. Davydova and Yu. Z. Danyushevskii, *Diode Generators and Microwave Amplifiers* (Radio Svyaz', Moscow, 1986) [in Russian].
- N. S. Boltovets, V. V. Kholevchuk, R. V. Konakova, V. F. Mitin, and E. F. Venger, Sens. Actuators, A **92**, 191 (2001).
- V. N. Alfeev, *Semiconductors, Superconductors and Paraelectrics in Cryoelectronics: Properties and Applications*

- in *Cryo electronic Integrated Circuits and Devices of Structures Based on Contacts of Semiconductors, Superconductors and Paraelectrics* (Sov. Radio, Moscow, 1979) [in Russian].
11. A. E. Belyaev, N. S. Boltovets, V. P. Klad'ko, R. V. Konakova, O. I. Lyubchenko, A. V. Sachenko, N. V. Safryuk, V. V. Shinkarenko, V. A. Pilipenko, T. V. Petlitskaya, A. A. Khodin, and P. N. Romanets, in *Proceedings of the 6th International Conference on Structural Relaxation in Solids, Vinnitsa, Ukraina, 2018*, p. 213.
 12. V. P. Klad'ko, L. I. Datsenko, J. Bak-Misiuk, S. I. Olikhovskii, V. F. Machulin, I. V. Prokopenko, V. B. Molodkin, and Z. V. Maksimenko, *J. Phys. D: Appl. Phys.* **34**, A87 (2001).
 13. R. K. Kupka and W. A. Anderson, *J. Appl. Phys.* **69**, 3623 (1991).
 14. G. Brezeanu, C. Cabuz, D. Dascalu, and P. A. Dan, *Solid State Electron.* **30**, 527 (1987).
 15. D. K. Ferry, *Phys. Rev. B* **14**, 1605 (1976).
 16. A. V. Sachenko, A. E. Belyaev, N. S. Boltovets, R. V. Konakova, Ja. Ja. Kudryk, S. V. Novitski, V. N. Sheremet, J. Li, and S. A. Vitusevich, *J. Appl. Phys.* **111**, 083701 (2012).
 17. B. I. Boltaks, M. K. Bakhadyrkhanov, S. M. Gorodetskii, and G. S. Kulikov, *Compensated Silicon* (Nauka, Leningrad, 1972) [in Russian].
 18. M. S. Yunusov, *Physical Phenomena in Silicon Doped with Platinum Group Elements* (FAN, Tashkent, 1983) [in Russian].
 19. *Physics and Material Science of Semiconductors with Deep Levels*, Ed. by V. I. Fistul' (Metallurgiya, Moscow, 1987) [in Russian].
 20. V. I. Fistul', *Introduction to Semiconductor Physics* (Vyssh. Shkola, Moscow, 1984) [in Russian].
 21. R. Smith, *Semiconductors* (Cambridge Univ. Press, Cambridge, 1959).
 22. B. I. Boltaks, *Diffusion and Point Defects in Semiconductors* (Nauka, Leningrad, 1972) [in Russian].
 23. S. S. Gorelik and M. Ya. Dashevskii, *Material Science of Semiconductors and Insulators* (Metallurgiya, Moscow, 1988) [in Russian].
 24. V. T. Bublik, S. Yu. Matsnev, K. D. Shcherbachev, M. V. Mezhennyi, M. G. Mil'vidskii, and V. Ya. Reznik, *Phys. Solid State* **45**, 1918 (2003).
 25. K. Ravi, *Impurities and Impurities in Semiconductor Silicon* (Wiley, New York, 1981).
 26. V. S. Vasil'ev, V. F. Kiselev, and B. N. Mukashev, *Defects in the Bulk and at the Surface of Silicon* (Nauka, Moscow, 1990) [in Russian].
 27. M. G. Mil'vidskii and V. B. Osvenskii, *Structural Defects in Single Crystal Semiconductors* (Metallurgiya, Moscow, 1984) [in Russian].
 28. A. Dargys and J. Kundrotas, *Handbook on Physical Properties of Ge, Si, GaAs and InP* (Science and Encyclopedia, Vilnius, 1994).

Translated by N. Korovin

SPELL: OK